The tethered motor domain of a kinesin-microtubule complex catalyzes reversible synthesis of bound ATP

David D. Hackney*

Department of Biological Sciences, Carnegie Mellon University, Pittsburgh, PA 15213

Edited by Edwin W. Taylor, Northwestern University Feinberg School of Medicine, Chicago, IL, and approved October 25, 2005 (received for review June 23, 2005)

Although the steps for the forward reaction of ATP hydrolysis by the motor protein kinesin have been studied extensively, the rates for the reverse reactions and thus the energy changes at each step are not as well defined. Oxygen isotopic exchange between water and P_i was used to evaluate the reverse rates. The fraction of the kinesin·ADP·P_i complex that reverts to ATP before release of P_i during net hydrolysis was ≈0 and ≈2.6% in the absence and presence of microtubules (MTs), respectively. The rate of synthesis of bound ATP from free P_i and the MT·kinesin·ADP complex was ≈1.7 $M^{-1}·s^{-1}$ ($K_{0.5}$ ADP = 70 μM) with monomeric kinesin in the absence of net hydrolysis. Synthesis of bound ATP from the ADP of the tethered head of a dimer–MT complex was 20-fold faster than for the monomer–MT complex. This MT-activated ATP synthesis at the tethered head is in marked contrast to the lack of MT stimulation of ADP release from the same site. The more rapid ATP synthesis with dimers suggests that the tethered head binds behind the strongly attached head, because this positions the neck linker of the tethered head toward the plus end of the MT and would thus facilitate its docking on synthesis of ATP. The observed rate of ATP synthesis also puts limits on the overall energetics that suggest that a significant fraction of the free energy of ATP hydrolysis is available to drive the docking of the neck linker on binding of ATP.

ATPase | energy coupling | motility | motor protein | isotopic exchange

Kinesin-1 is molecular motor that moves along microtubules (MTs) in a highly processive manner. Scheme 1 presents a minimal mechanism for ATP hydrolysis by the MT complex of a kinesin monomer motor domain (see refs. 1–3 for recent reviews of the ATPase mechanism and coupling to motility). ATP binds rapidly and is hydrolyzed at 100–300 s^{-1}. P_i release occurs without a lag after hydrolysis, and thus P_i release is at least as fast as hydrolysis ($k_3 \geq k_2$). ADP release is partially rate-limiting for conventional kinesin-1 and may be the principal rate limiting step for some other kinesin superfamily members.

Another important aspect, however, is the equilibrium constant of each step, because it determines the free energy that is available at that step for coupling to movement against a load. The equilibrium constants can be determined if the rates in the reverse direction are known, but this is difficult because the overall equilibrium strongly favors hydrolysis. Oxygen isotopic exchange is a powerful technique for evaluation of the reversibility of the hydrolysis reaction and has provided important insight into the mechanism of the F1-ATPase (4) and myosin (5, 6). It is used here to determine the rates of the reverse reactions of kinesin.

Hydrolysis of ATP by kinesin proceeds through attack of water on the γ phosphoryl to yield P_i that contains one water-derived oxygen and three oxygens from the nonbridge γ oxygens of the ATP, as indicated in Scheme 2 for hydrolysis of unenriched ATP in 100% ^{18}O-enriched water. If P_i release via k_3 is much faster than resynthesis of ATP via k_{-2}, then the released P_i will have one and only one water-derived ^{18}O oxygen. If reversal to reform ATP does occur, then the ATP that is formed will retain the water-derived ^{18}O oxygen 75% of the time for a random process. Rehydrolysis of this recycled ATP generates a bound P_i with two water-derived ^{18}O oxygens. Subsequent reversals can incorporate additional oxygens. The partition coefficient (P_c) = $k_{-2}/(k_{-2} + k_3)$ gives the fraction the E·ADP·P_i complex that reforms E·ATP, and it can be determined by statistical analysis of the distribution of P_i with labeled ^{18}O oxygens (7). In addition to this intermediate exchange that occurs during net ATP hydrolysis, medium exchange reactions can occur by reversal from free species. In particular, medium P_i = water exchange as indicated in Scheme 3 monitors the reformation of bound ATP from bound ADP and free P_i in the medium.

The analysis of these exchange reactions reported here provides an evaluation of key rates in the reverse direction that allow the overall energy profile of the MT-activated kinesin ATPase cycle to be established. In addition, the striking difference between monomeric and dimeric constructs indicates that the tethered head of a dimer is able to bind to the MT in a mode that is competent for resynthesis of ATP at a rate 20-fold greater than for monomers.

Materials and Methods

DKH346 and DKH405 are monomer and dimer motor domains of conventional *Drosophila* kinesin-1 (8). BKinM is DKH346 fused at the N terminus to the N-terminal extension of BimC (9), a member of the kinesin-5 family. The plasmid for expression of monomeric human K349 (10) was a gift of R. Vale (University of California, San Francisco). K349 was used in studies of nucleotide-free kinesin, because human kinesin is more stable than *Drosophila* kinesin in the absence of bound nucleotide. MTs were prepared from porcine tubulin and stabilized with paclitaxel, as described (11), and the concentration of MTs is expressed as the concentration of tubulin heterodimers. Reactions were conducted at 25°C in A25 buffer (12) with 25 mM KCl. Stopped-flow analysis of the binding of 2′(3′)-*O*-(*N*-methylanthraniloyl)ADP to kinesin was determined as described (11), with excitation at 285 nm.

Exchange Methods. ^{18}O-enriched P_i for medium exchange reactions was synthesized by reaction of phosphorus pentachloride and enriched water, as described (7). Intermediate exchange was analyzed by hydrolysis of 1 mM unenriched ATP in 75–80% [^{18}O]water with pyruvate kinase and 4 mM phosphoenolpyruvate to regenerate ATP. Reactions were quenched with HCl after ≈90% consumption of phosphoenolpyruvate and the distribution of P_i species containing 0, 1, 2, 3, or 4 ^{18}O-oxygens per P_i was determined by gas chromatography/mass spectrometry after conversion of the P_i to volatile triethyl P_i, essentially as described (13). Typical data and analysis for the intermediate exchange of DKH346 with and without MTs in ^{18}O-water are

Conflict of interest statement: No conflicts declared.

This paper was submitted directly (Track II) to the PNAS office.

Abbreviations: P_c, partition coefficient; MT, microtubule; NL, neck linker.

*E-mail: ddh@andrew.cmu.edu.

Scheme 1. Minimal scheme for hydrolysis of ATP by the complex of kinesin (E) with MTs.

given in Table 2 (see *Supporting Text* and Table 2, which are published as supporting information on the PNAS web site).

The extent of the medium exchange reactions was determined by fitting the increase in the ratio of the $^{18}O_3$:$^{18}O_4$ species versus time to the full theoretical model (7, 14) by using a low ratio of k_{-2}/k_3. The calculated amount of exchange is insensitive to the exact k_{-2}/k_3 ratio as long as it is small enough that multiple reversals of the hydrolysis step during each cycle are rare. Exchange rates are reported as the rate of incorporation of water-derived oxygens into P_i, which is equal to the rate of synthesis of ATP for Scheme 3.

Thermodynamic Calculations. The $\Delta G°$ apparent for ATP hydrolysis at 25°C, 1 mM Mg^{2+}, and $\mu = 0.20–0.25$ is estimated by Metzler (15) as -30.35 kJ/mol at pH 7 and by Alberty (16) as -32.49 kJ/mol at $[H^+] = 10^{-7}$ M, which corresponds to a pH of 7.14 based on activity of H^+. A value of -31.4 kJ/mol was assumed in the calculations presented here for A25 buffer with 25 mM KCl at pH 6.9, ≈1.9 mM Mg^{2+}, and $\mu = \approx 0.05$.

Results and Discussion

Determination of P_c from Intermediate Exchange During Net Hydrolysis. Initial exchange experiments with ^{18}O-labeled ATP in unenriched water established that the P_c value was small for the MT-activated ATPase of kinesin (17), but the amount of exchange was too close to the level of detection for accurate evaluation, because the [^{18}O]phosphoenolpyruvate that was used to generate the ATP was not of high enrichment. Hydrolysis of unenriched ATP in 80% ^{18}O-enriched water provides a more accurate measurement of P_c at low levels of exchange. P_c values obtained in this way during net steady-state hydrolysis are summarized in Table 1, with detailed distributions given in Table 2. In the absence of MTs, the P_c value is indistinguishable from zero, indicating that almost no reversal of Step 2 occurs during turnover, and thus either P_i release (k_3) is extremely rapid or ATP resynthesis (k_{-2}) is extremely slow, or both. In the presence of MTs, both monomeric and dimeric constructs have P_c values of ≈2.6%, indicating a small, but significant, amount of reversal of the ATP hydrolysis reaction (Step 2). It is interesting to note that this is the exact opposite of the pattern for myosin. In the absence of actin, myosin has a high basal P_c value with extensive resynthesis of ATP that is decreased by actin (see ref. 5).

A P_c value does not uniquely define the rate of ATP synthesis (k_{-2}) or the equilibrium constant for hydrolysis of bound ATP (K_2), because the exact value of k_3 is not known, but it does impose model-dependent limits. This is important, because the equilibrium constant for ATP hydrolysis was believed to favor products, but an upper limit on K_2 was not known and thus Step 2 could potentially have had a large negative ΔG value. For $P_c = k_{-2}/(k_{-2} + k_3) = 2.6\%$, P_c will equal $\approx k_{-2}/k_3$ (because $k_{-2} \ll k_3$), and k_{-2} will be ≈2.6% k_3. If P_i release is faster than ATP hydrolysis ($k_3 > k_2$), then k_{-2} will be >2.6% of k_2, and thus $K_2 = k_2\, k_{-2} \leq k_2/(0.026\, k_2) \leq 39$. This analysis suggests that K_2 does favor formation of the hydrolysis products but not by a large enough amount to constitute a major part of the total free energy drop.

Two factors may cause the observed rate of exchange to underestimate the true extent of reversal of hydrolysis. One is that observation of isotopic exchange depends on the bound P_i being able to randomize its oxygens atoms before reversal to reform ATP. Otherwise, the same water-derived oxygen that had been incorporated during hydrolysis would be preferentially returned to the water pool on resynthesis of ATP. This would result in a reversal of Step 2 that was "isotopically silent" and would not contribute to the observed rate and resulting P_c value. Similarly, the water that is released by reversal of hydrolysis must be free to rapidly equilibrate with the bulk water. Most previous studies have not indicated such limitation, but the short lifetime of the state with bound P_i in the case of kinesin may preclude complete randomization. To the extent that these factors contribute, however, they would cause underestimation of the true k_{-2} value and would mean that K_2 is even smaller than the above estimate.

Rate of Reversible ATP Synthesis from Free P_i by Monomeric BKinM. The rate of ATP synthesis from free P_i by reversal of Steps 2 and 3 can be determined from the rate of loss of ^{18}O oxygens from P_i in unlabeled water, as indicated in Scheme 3. Analysis of the fully MT-activated process is difficult to achieve with monomer motor domains, because their net affinity for MTs is weak in the presence of saturating ADP levels. This difficulty can be overcome by the use of BKinM (9). This construct consists of the full-length monomer motor domain of DKH346 fused to the N-terminal extension of BimC, which loosely tethers the motor domain to the MT with greatly increased net MT affinity but without perturbation of the ATPase rate or sliding velocity (9). The exchange reaction occurs slowly, but its rate is approxi-

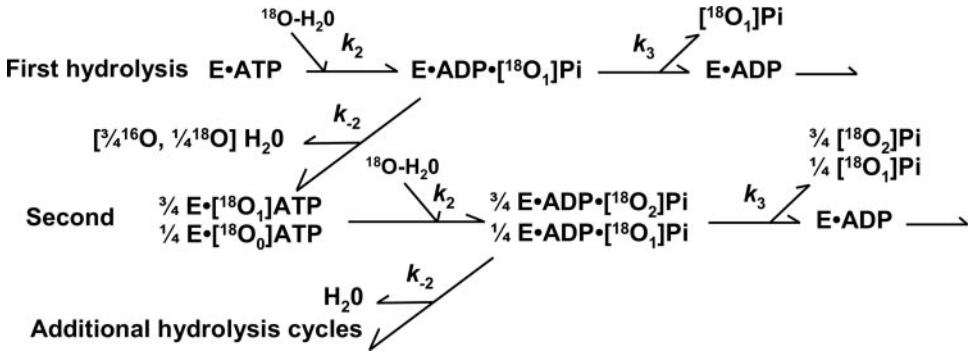

Scheme 2. Mechanism for intermediate exchange during net hydrolysis.

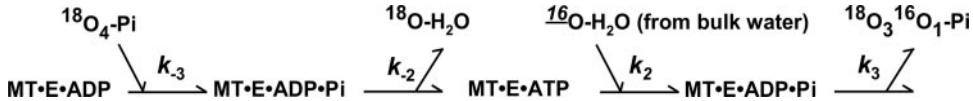

Scheme 3. Mechanism for exchange of water-derived oxygens into P_i of the medium by reversible synthesis of bound ATP. Note that reversible formation of a pentacoordinate intermediate from ADP and P_i would not produce exchange with water, because no dehydration occurs until ATP is formed. Exchange could in principle occur by reversible dehydration of P_i to generate metaphosphate without formation of ATP. Metaphosphate, however, would be a highly unstable intermediate that would likely have an energy close to that for the transition state leading to ATP synthesis, and thus both processes would be expected to have similar rates. Also, exchange by a metaphosphate route would require equilibration of the released water with the bulk water pool during the extremely short lifetime of this unstable intermediate, rather than during the much longer lifetime of the ATP state.

mately linear, as indicated in Fig. 1*a* for the increase in P_i with only three ^{18}O oxygens with time (with greater extents of exchange, curvature is expected due to accumulation of P_i with more than one water-derived oxygen). Omission of either MTs, ADP, or BKinM eliminates the exchange reaction. The $K_{0.5}$ for half saturation with ADP in the reverse reaction is 70 μM (Fig. 1*b*), and the exchange rate scales linearly with [P_i] (Fig. 1*c*), as expected for weak P_i binding. The net bimolecular rate for reversal of Steps 2 and 3 to reform ATP at 1 mM ADP and 0.5–1.0 mM P_i was 1.73 ± 0.34 $M^{-1}{\cdot}s^{-1}$ (SD, $n = 6$). The BimC fusion does not influence the rate, because a similar value of 2.2 $M^{-1}{\cdot}s^{-1}$ was obtained with unmodified DKH346 at 30 μM MTs and 8 mM KCl, where MT binding is largely saturated.

P_i Dissociation Constant. The rate of ATP resynthesis by monomers suggests that productive P_i binding to the ternary complex of kinesin with MTs and ADP is weak. If P_i release is not rate limiting with $k_3 \geq 200\ s^{-1}$, then k_{-2} is $\geq 5\ s^{-1}$, because $P_c = \approx k_{-2}/k_3 = 2.6\%$. For Step 3 in rapid equilibrium compared with reversal of Step 2, the bimolecular rate constant at low [P_i] for synthesis of ATP will be $k_{-2}/K_3 = 1.7\ M^{-1}{\cdot}s^{-1}$, and thus $K_3 \geq 3$ M. Note that the analogous estimate of K_3 for kinesin dimers will be lower, because their exchange rate is faster, as indicated below, but K_3 will still be weak at ≥150 mM.

It should be emphasized that the value of K_3 estimated in this way is for formation of the P_i state that immediately follows hydrolysis, and therefore K_3 is not necessarily equal to the observed K_d for P_i binding. In particular, P_i binding by reverse of Step 3 is unlikely to be a single process when analyzed in detail and may consist of initial reversible binding of P_i followed by a conformational change to form the quaternary complex that directly undergoes dehydration in Step 2. Consequently, K_d and K_3 can differ. For example, a K_d of 300 mM for initial P_i binding to MT·E·ADP followed by an unfavorable conformational change with an equilibrium constant of 0.1 would also yield a net K_3 value of ≈3 M.

There have been several observations of effects of added P_i with a $K_{0.5}$ in the low-mM range (18–20). These have been interpreted as being due to reversal of Step 3 to form the quaternary MT·E·ADP·P_i complex, but the exchange reactions suggest Pi binding may be weaker in this mode. A possible resolution is that nucleotide-free kinesin binds P_i in the low-mM range in a mode that inhibits ADP binding, as indicated in Fig. 2. The monoanions chloride and acetate (not shown) do not produce inhibition, but sulfate is an even more effective inhibitor than P_i. Further work will be required to tell whether this is due to binding of P_i at the γ or β phosphoryl subsites or to an allosteric site [as observed for much weaker allosteric binding to E·ADP (21)], but the critical result is that P_i binding to nucleotide-free kinesin is antagonistic to ADP binding. An important aspect of the medium-exchange reaction studied here is that it is sensitive only to productive binding of Pi to MT·E·ADP (e.g., true reversal of Steps 2 and 3) and is not influenced by P_i binding to the nucleotide-free MT·E complex in the presence of high concentrations of ADP.

Table 1. Exchange during hydrolysis

Construct	Pc, % (−)MTs	Pc, % (+)MTs
DKH346	<0.2	2.57 ± 0.28
DKH405	<0.2	2.78 ± 0.32
BKinM	<0.2	2.52 ± 0.20

Rate of Reversible ATP Synthesis from Free P_i by Dimeric DKH405. Unexpectedly, dimeric DKH405 catalyzes ATP synthesis at a rate that is greatly accelerated over that for monomers, as indicated in Fig. 1*d*, with some inactivation over long times. Furthermore, the reaction with DKH405 is saturated at 2 μM free ADP with no further increase at 3 or 5 μM ADP, unlike the monomer reaction that requires 70 μM ADP for half saturation. The rate for reversal of Steps 2 and 3 to reform ATP at 2 μM free ADP and 1.0 mM P_i was determined after 30 min of reaction to avoid inactivation and was 17.0 ± 3.9 $M^{-1}{\cdot}s^{-1}$ (SD, $n = 5$) per head or 34 $M^{-1}{\cdot}s^{-1}$ per dimer. The acceleration with dimeric DKH405 over that with monomeric BKinM is likely related to the nature of the tethered intermediate that is produced by dimers, but not monomers, on binding to MTs, as indicated in Scheme 4. With monomers, ADP binding to the MT complex is weak (70 μM, Fig. 1*b*) due to rapid ADP release (>100 s^{-1}). When dimeric kinesin binds to a MT, it releases half of its bound ADP to form a tethered intermediate with one head retaining its ADP, whereas the other head releases its ADP and becomes tightly attached to the MT (22). The head with ADP remains tethered to the MT by the strongly attached head, but constraints in the dimer prevent the tethered head from interacting with the MT in a way that can stimulate ADP release. Resynthesis of ATP by dimers therefore likely occurs on the tethered head, because it is fully saturated for DKH405 even at 1 μM ADP (11), whereas the strongly attached head binds ADP weakly. Reversible synthesis of ATP at the tethered head establishes that reversible ATP hydrolysis can occur in the absence of nucleotide at the strongly attached head. This in turn suggests that ADP release from the lead head may precede or occur in parallel with hydrolysis on the trailing head in the major pathway (see ref. 11 for discussion of the implications of the relative rate of hydrolysis and ADP release for processivity).

The rate of ATP synthesis will be equal to the rate of P_i binding (k_{-3}) times the fraction of the bound P_i that goes on to ATP. This fraction is the P_c value of $k_{-2}/(k_{-2} + k_3)$, and thus the ATP synthesis rate equals $k_{-3}\,P_c$. Because P_c is the same for monomers and dimers, this indicated that the 20-fold increase in rate with dimers is principally due to a faster rate of P_i binding. This does not necessarily mean that the K_d for P_i in Step 3 is lower for dimers, because k_{-2} and k_3 could have changed in parallel while maintaining the same P_c value. Also, the P_c value with dimers was determined during rapid cycling at high [ATP], whereas the medium exchange was determined with the ATP-waiting state.

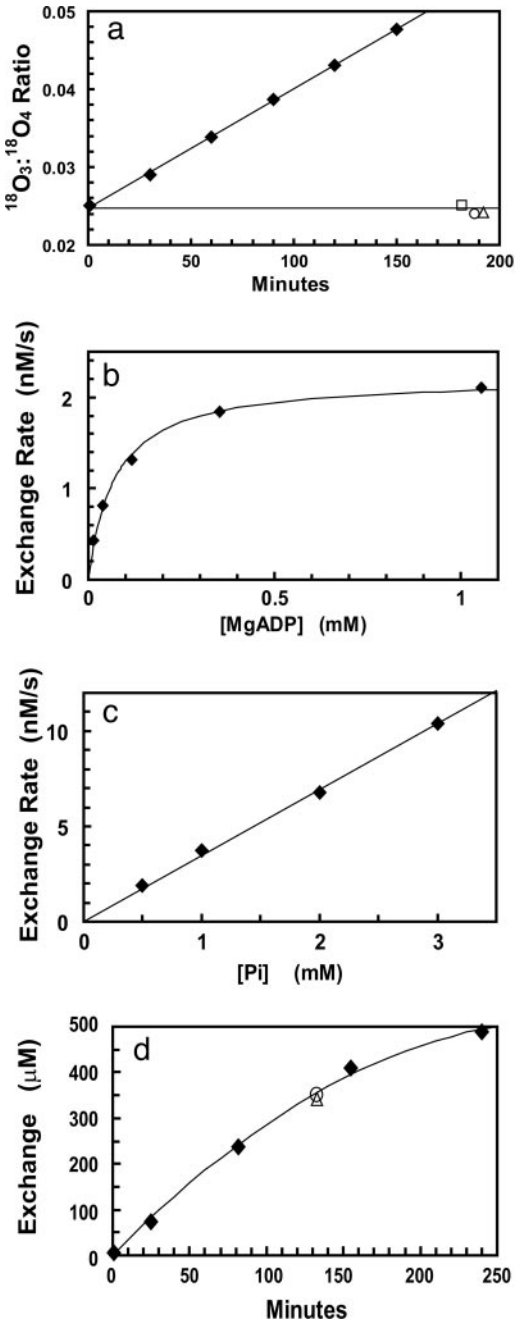

Fig. 1. Medium P_i = water oxygen exchange by kinesin. (*a*) Change in ratio of $^{18}O_3$-P_i:$^{18}O_4$-P_i species versus time for monomeric BKinM. Full reaction with 2 μM BKinM, 4 μM MTs, 1 mM MgADP, and 1 mM ^{18}O-P_i (diamonds). Control reactions had one component omitted. Minus MTs (square), minus ADP (circle), and minus BKinM (triangle). (*b*) Dependence of exchange rate on [ADP]. As in *a*, except for 0.5 mM P_i and variation in [ADP]. Reaction for 154 min. A K_d of 70 μM was determined by fitting to a hyperbolic binding model. (*c*) Dependence of exchange rate on [P_i]. As in *a* at 1 mM MgADP and variable [P_i]. Reaction for 168 min. (*d*) Progress of exchange reaction for dimeric DKH405. Reaction as 2 μM DKH405 (per head concentration), 4 μM MTs, and 1 mM ^{18}O-P_i. No ADP was added, and the free [ADP] was 2 μM that resulted from half-site release of ADP on binding of DKH405 to the MT and from carryover of free ADP in the stock of DKH405. Control reactions had extra ADP added to a total free concentration of 3 μM (circle) or 5 μM (triangle). Results are reported as total amount of exchange, because the exchange is more extensive than in *a* with multiple cycles of exchange having occurred. Consequently, the $^{18}O_3$-P_i:$^{18}O_4$-P_i ratio no longer scales linearly with the amount of exchange. For comparison, the point at 25 min has a $^{18}O_3$-P_i:$^{18}O_4$-P_i ratio of 0.097 that is already off the scale of *a*.

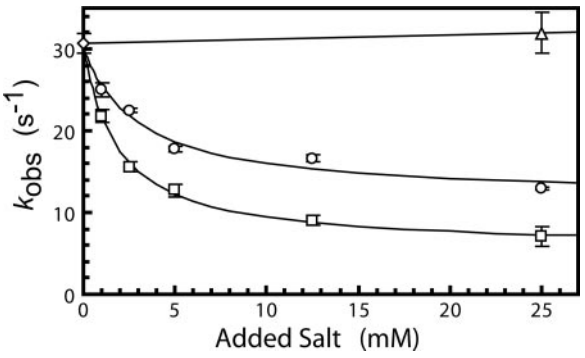

Fig. 2. Influence of added salts on binding of 2′(3′)-*O*-(*N*-methylanthraniloyl)ADP (mantADP) to nucleotide-free K349. Stopped-flow analysis of the rate of the fluorescent transient on binding of mantADP to nucleotide-free human K349 monomer. Final concentrations of 0.24 μM K349 and 2.9 μM mantADP in A25 buffer with 25 mM KCl plus additional potassium salts as indicated. No addition, diamond; P_i, circles; sulfate, squares; KCl to 50 mM total, triangle. Hyperbolic fits to data yield $K_{0.5}$ values of 3.1 and 1.8 mM and maximum fractional inhibitions of 61 and 81% for P_i and sulfate, respectively.

Implications for Conformation of the Tethered Intermediate. The tethered head of a dimer is able to interact with the MT in a manner that not only stimulates the synthesis of ATP but also accelerates it another 20-fold over the reaction catalyzed by the monomer–MT complex. This is in striking contrast to the >2,000-fold inhibition of ADP release from >100 to 0.05 s^{-1} (11) from the same active site of the tethered head. Interaction of the tethered head with the MT is also consistent with the lack of mobility of the tethered head seen previously (23). Possible conformations for MT-bound monomers and tethered dimers are given in Scheme 4 as a framework for discussion of the implications of the exchange results. A key structural feature is the neck linker (NL) that connects the core motor domain to the neck coil (dimerization domain indicated by paired lines) and the more distal cargo-binding region. Rice *et al.* (24) showed that the NL is disordered (or present in multiple discrete conformations) when monomer motor domains are bound to the MT in the absence or presence of ADP, but in the presence of the nonhydrolyzable ATP analog AMP-PNP, the NL becomes attached to the motor domain and is directed toward the plus end of the MT. Cryoelectron microscopy results have also indicated that the NL is disordered in the nucleotide-free state (25). The undocked conformations of the NL are indicated by multiple curved lines for the monomer in Scheme 4, whereas the docked conformation in the presence of ATP is indicated by the straight arrow pointing toward the plus end of the MT. Because the neck coil is connected to the end of the NL (the pointed head of the arrow), transition from the undocked to the docked conformation on ATP binding moves the average position of the end of the NL and attached cargo toward the plus end, and this transition is likely an important aspect of how kinesin generates movement.

Which of the possible conformations of the tethered intermediate in Scheme 4 are most compatible with the exchange results? Conformations such as C cannot have either rapid MT-stimulated ADP release or ATP synthesis for the trivial reason that the tethered head is not bound to the MT. In state E, the docking of the NL of the lead head on ATP resynthesis would be inhibited, because it would force uncoiling of the neck coil or other energetically unfavorable changes to accommodate the increased spacing between the ends of the NLs. Binding of the tethered head in the trailing location as in B, however, would position the NL in the forward direction that is required for docking of the NL on ATP binding (24), and that should also occur on ATP synthesis. This would be advantageous for two reasons. One is that the undocked NL of a monomer in A is free to adopt a range of conformations,

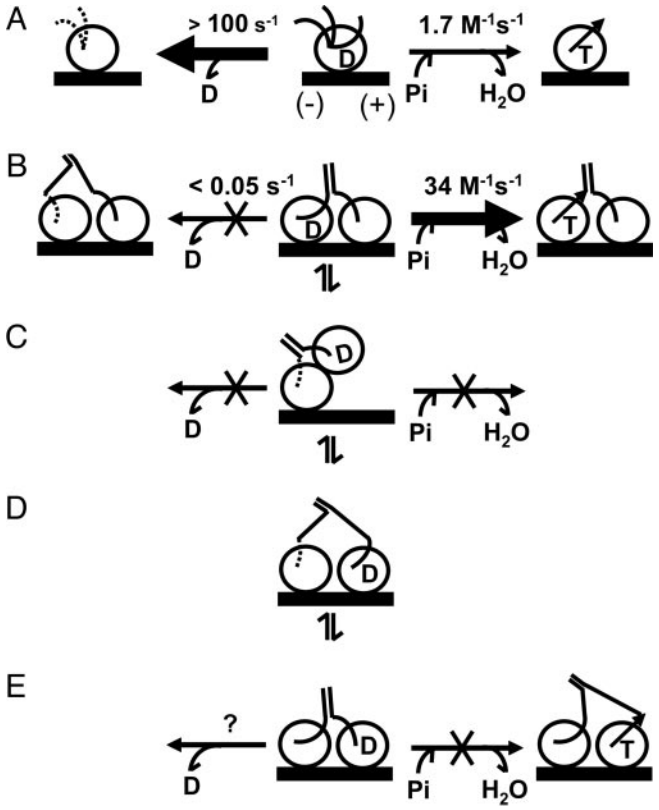

Scheme 4. Comparison of ADP release and ATP resynthesis by monomers and the tethered head of a kinesin dimer bound to a MT. Motor domains are represented by circles with the MT indicated by a solid bar with the plus end at the right. ADP and ATP are indicated by D and T, respectively, with the three species on each line being the nucleotide-free, ADP, and ATP forms. The NL is indicated by a line originating near position of I325 (human kinesin numbering) with a curved line depicting an undocked linker and a straight arrow indicating the forward directed position of the docked linker in the presence of ATP (see ref. 2 for a more complete description of this schematic representation). The increased freedom of the undocked NL with monomers is indicated by the multiple conformations of the NL in A. An intact neck coil is indicted by long parallel lines, and a partially uncoiled neck coil is indicated by shorter parallel lines and single lines leading to the ends of the NLs. The weight of the arrows in lines A and B is only intended to convey the relative changes in rate between monomers and dimers for each step. As discussed in the text, the equilibrium for ATP synthesis still strongly favors hydrolysis at 1 mM P_i even for dimers.

only some of which are favorable for linker docking, whereas the tethered dimer in B avoids at least some unfavorable orientations. The other is that the undocked NL is an entropic spring that will be contracted in an undocked monomer and must be extended to form the docked conformation. In state B, however, the entropic spring of the NL of the tethered head is at least partially preextended in approximately the correct direction, and this results in a lower energy barrier to docking of the linker. It is also possible that the true rate of ATP synthesis from B is faster than 34 $M^{-1}{\cdot}s^{-1}$, and that the observed rate is reduced from its maximum value because significant amounts of other states such as C are in equilibrium with B. These considerations also suggest that both the ATP and the ADP+P_i state are docked in the dimer, if the principal cause of the acceleration of ATP synthesis with dimers is an increase in k_{-3} as discussed above.

Asenjo *et al.* (23) have noted that if the tethered head was docked as in state B and if ADP release required a backwards orientation of the NL, then ADP release would be inhibited from the tethered head, as indicated in Scheme 4B, because of the need to introduce

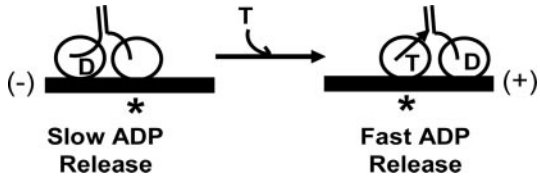

Scheme 5. Model for ATP-induced movement of the tethered head from the rear to the lead position. The starting configuration is that of B in Scheme 4 that is consistent with the acceleration of medium P_i = water exchange with dimers. ATP binding to the lead head would favor NL docking, and this would displace the trailing head with ADP toward the lead position with stimulation of ADP release. * marks a fixed position on the MT.

strain to accommodate a rearward orientation. However, ADP release would be accelerated after ATP-induced NL docking and coupled movement of the tethered head to the forward position as in Scheme 5. Skiniotis *et al.* (25) have also noted the likely importance of the asymmetry introduced in a bound dimer by having the NL on the leading head directed backwards, whereas the reverse is true for the trailing head. The stimulation of ATP synthesis reported here suggests that docking of the tethered head in State B does occur at least in part and thus supports the model in Scheme 5. Significantly, State B is also the one expected to be favored by application of a load directed toward the rear (2).

Although ATP is stabilized at the tethered head, the overall equilibrium between bound ATP and bound ADP plus free P_i still strongly favors the ADP form at 1 mM P_i. Thus the tethered head, although potentially bound as in B, would usually be in the weakly interacting ADP form and could be easily dissociated from the MT during the transition in Scheme 5. One apparent conflict is that this model also suggests that ADP release should be rapid from state E, because the NL of the head with ADP is directed toward the rear, but state E may be poorly populated, because it is more correctly represented by state D, which explicitly considers the unfavorable rearward orientation of the NL on the nucleotide-free head.

A puzzling aspect of the kinetics of constructs having spacers inserted between the NL and neck coil was that only very long spacers were effective in accelerating ADP release from the tethered head (26). Inserts of 12 amino acids (six on each head of a dimer) accelerated ADP release to only 4 s^{-1} and inserts of twice this length released ADP at just 35 s^{-1}, which is still less than the ATP-stimulated rate for unmodified DKH405. The model of Scheme 4B would provide a simple explanation for this requirement, because a separation of up to 8 nm could potentially be required for rapid ADP release if both NLs had to be directed toward the rear. Only very long inserts would be able to span this gap without significant entropic strain.

Implications for Energetics. Determination of the rate of ATP synthesis allows limits to be placed on the energy changes at each step. The net ΔG for hydrolysis is -55 kJ/mol for approximate physiological values of 1, 0.07, and 1 mM for ATP, ADP, and P_i, respectively. The rate of hydrolysis and coupled P_i release via Steps 2 and 3 is likely 100–300 s^{-1} (see refs. 1 and 2), and thus the net equilibrium constant for Steps 2 and 3 for dimeric DKH405 is $K_{2,3} = \approx 200\ s^{-1}/34\ M^{-1}{\cdot}s^{-1} = 6$ M and has a ΔG of -21.5 kJ/mol at 1 mM P_i. There is little net ΔG associated with ADP release, because the K_d for ADP is close to the physiological concentration (at least for monomeric BKinM above), and thus the ΔG for ATP binding in Step 1 at 1 mM ATP is -33.6 kJ/mol by difference. For two-step binding of ATP with an initial rapid equilibrium followed by a conformational change, a K_d of 0.1 mM for formation of an initial complex would leave -27.9 kJ/mol for an ATP-induced conformational change. This ΔG is equivalent to the 24–34 kJ/mol required to drive a full 8-nm step against a stall force of 5–7 pN. Even if there was some

rate limitation due to a conformational change before hydrolysis (27, 28), and the true hydrolysis rate was faster, the ΔG for the ATP-induced conformational change would still be -18.2 kJ/mol at an effective rate of 10,000 s^{-1} for hydrolysis and P_i release.

It should also be noted that the ΔG of 24–34 kJ/mol that produces stall is less than the 55 kJ/mol for hydrolysis used above and much less than the effective ΔG during motility assays in the absence of added ADP or P_i. Thus stall is not an equilibrium state, as observed with F1 ATPase (29, 30), and the backward steps that are observed at high load with kinesin (31, 32) are not due to simple reversal of the forward reaction.

One difficulty with the model of Rice *et al.* (24) for docking of the NL as the principal step that produced net movement was that the previous measurement of 3 kJ/mol for ATP-induced NL docking (using AMP-PNP as a nonhydrolyzable analog of ATP) was too small to drive movement against a load (33). However, the analysis presented here, without use of analogs, demonstrates that a significant part of the energy of hydrolysis is likely available in the region of Step 1 to drive the forward movement of the NL against a load.

I thank M. Stock and E. Rruka for isolation of proteins; W. Brown and G. Lowey for mass spectrometer use; and W. McClure, E. De La Cruz, and T. Shimizu for helpful comments on the manuscript. This work was supported by National Institutes of Health Grant NS28562.

1. Cross, R. A. (2004) *Trends Biochem. Sci.* **29,** 301–309.
2. Hackney, D. D. (2003) in *The Enzymes*, eds. Hackney, D. D. & Tamanoi, F. (Academic, San Diego), Vol. 23, pp. 88–143.
3. Hancock, W. O. & Howard, J. (2003) in *Molecular Motors*, ed. Schliwa, M. (Wiley-VCH, New York), pp. 243–269.
4. Boyer, P. D. (1993) *Biochim. Biophys. Acta* **1140,** 215–250.
5. Sleep, J. A., Hackney, D. D. & Boyer, P. D. (1980) *J. Biol. Chem.* **255,** 4097–4099.
6. Webb, M. R., Hibberd, M. G., Goldman, Y. E. & Trentham, D. R. (1986) *J. Biol. Chem.* **261,** 15557–15564.
7. Hackney, D. D., Stempel, K. E. & Boyer, P. D. (1980) *Methods Enzymol.* **64,** 60–83.
8. Jiang, W., Stock, M., Li, X. & Hackney, D. D. (1997) *J. Biol. Chem.* **272,** 7626–7632.
9. Stock, M. F., Chu, J. & Hackney, D. D. (2003) *J. Biol. Chem.* **278,** 52315–52322.
10. Kull, R. J., Sablin, E. P., Lau, R., Fletterick, R. J. & Vale, R. D. (1996) *Nature* **380,** 550–555.
11. Hackney, D. D. (2002) *Biochemistry* **41,** 4437–4446.
12. Huang, T. G. & Hackney, D. D. (1994) *J. Biol. Chem.* **269,** 16493–16501.
13. Dale, M. P. & Hackney, D. D. (1987) *Biochemistry* **26,** 8365–8372.
14. Hackney, D. D. (1980) *J. Biol. Chem.* **255,** 5320–5328.
15. Metzler, D. E. (2001) in *Biochemistry* (Academic, San Diego), p. 296.
16. Alberty, R. A. (2003) *Thermodynamics of Biochemical Reactions* (Wiley International, Hoboken, NJ).
17. Hackney, D. D. (1988) *Proc. Natl. Acad. Sci. USA* **85,** 6314–6318.
18. Rosenfeld, S. S., Rener, B., Correia, J. J., Mayo, M. S. & Cheung, H. C. (1996) *J. Biol. Chem.* **271,** 9473–9482.
19. Schief, W. R., Clark, R. H., Crevenna, A. H. & Howard, J. (2004) *Proc. Natl. Acad. Sci. USA* **101,** 1183–1188.
20. Crevel, I. M., Nyitrai, M., Alonso, M. C., Weiss, S., Geeves, M. A. & Cross, R. A. (2004) *EMBO J.* **23,** 23–32.
21. Sindelar, C. V., Budny, M. J., Rice, S., Naber, N., Fletterick, R. & Cooke, R. (2002) *Nat. Struct. Biol.* **9,** 844–848.
22. Hackney, D. D. (1994) *Proc. Natl. Acad. Sci. USA* **91,** 6865–6869.
23. Asenjo, A. B., Krohn, N. & Sosa, H. (2003) *Nat. Struct. Biol.* **10,** 836–842.
24. Rice, S., Lin, A. W., Safer, D., Hart, C. L., Naber, N., Carragher, B. O., Cain, S. M., Pechatnikova, E., Wilson-Kubalek, E. M., Whittaker, M., *et al.* (1999) *Nature* **402,** 778–784.
25. Skiniotis, G., Surrey, T., Altmann, S., Gross, H., Song, Y. H., Mandelkow, E. & Hoenger, A. (2003) *EMBO J.* **22,** 1518–1528.
26. Hackney, D. D., Stock, M. F., Moore, J. & Patterson, R. A. (2003) *Biochemistry* **42,** 12011–12018.
27. Rosenfeld, S. S., Jefferson, G. M. & King, P. H. (2001) *J. Biol. Chem.* **276,** 40167–40174.
28. Geeves, M. A. & Holmes, K. C. (1999) *Annu. Rev. Biochem.* **68,** 687–728.
29. Kinosita, K., Jr., Yasuda, R., Noji, H. & Adachi, K. (2000) *Philos. Trans. R. Soc. London B* **355,** 473–489.
30. Itoh, H., Takahashi, A., Adachi, K., Noji, H., Yasuda, R., Yoshida, M. & Kinosita, K. (2004) *Nature* **427,** 465–468.
31. Nishiyama, M., Higuchi, H. & Yanagida, T. (2002) *Nat. Cell Biol.* **4,** 790–797.
32. Carter, N. J. & Cross, R. A. (2005) *Nature* **435,** 308–312.
33. Rice, S., Cui, Y., Sindelar, C., Naber, N., Matuska, M., Vale, R. & Cooke, R. (2003) *Biophys. J.* **84,** 1844–1854.